Tariff-driven demand side management of green ship

Zhou Wu[a,b], Xiaohua Xia[c]

[a]*Key Laboratory of Complex System Safety and Control (Chongqing University), Ministry of Education, China (Email: wuzhsky@gmail.com, Tel/Fax: +862365112173)*
[b]*School of Automation, Chongqing University, Chongqing, China*
[c]*Department of Electrical Electronic and Computer Engineering, University of Pretoria, Pretoria, South Africa (Email: xxia@up.ac.za)*

Abstract

Green ships with hybrid renewable energy systems become important resources of demand side management, when ships in port have the grid connection. Variance of electricity tariff has influenced the optimal solutions to power management. Current power management methods for stand-alone green ships cannot be applied to this new situation. To enable tariff-driven power management, a unified model is proposed for a green ship under different time-of-use (TOU) tariffs. In the proposed model, diesel generation, solar energy, and battery storage could support auxiliary power demand, and the surplus of solar energy could be sold to grid when the ship is connected to grid. A power flow dispatching problem is then formulated as the optimization of operational cost. To cope with variance of tariff, solar energy, and on-board load demand, a receding horizon control approach is employed to ensure a closed-loop control mechanism. Experimental results indicate the tariff-driven model can effectively reduce the overall cost of green ships, and the receding horizon control can improve the performance in terms of fuel consumption and greenhouse gas emission.

Keywords:
green ship, demand side managment, economic load dispatching, receding horizon control

1. Introduction

Over 90% of cargoes are transported by ships over the world, while greenhouse gas (GHG) emission and fossil fuel consumption are two critical problems in the shipping industry. In 2007, international shipping is responsible for approximately 3% global GHG emission, and 277 million tons of diesel/gasoline, in which the dry bulk shipping is the first contributor with about 52 million tons [1]. To suppress the continuous increase of GHG emission and fossil fuel demand in the international shipping, international maritime organization (IMO) has issued strict regulations for shipping energy efficiency and GHG emission. Therefore, green ship technologies become urgent to improve shipping energy efficiency and reduce GHG emission. One of the most popular technology is to find clean energy to take the place of fossil fuel [2]. Renewable energy (RE) resources have played increasingly significant roles to reduce fuel consumption and GHG emission in the green ship. Among available RE resources, solar energy is the most promising option of green ship, as solar is clean, safe, omnipresent, and freely available.

In general, photovoltaic (PV) panels have to be equipped together with storage components (battery, ultra-capacitor, and so on) for providing stable and sustainable power. Multiple renewable sources and storage components are usually combined in a hybrid renewable energy system (HRES). In the stand-alone application, e.g., remote communities, the HRES is able to supply electricity for off-grid customers [3, 4, 5, 6]. In the grid-connected application, e.g., the berthing green ship, the HRES can also serve as distributed generation to sell the surplus of renewable energy on grid, which can bring financial profits on the electricity market [7, 8, 9]. Researchers have studied many theoretical and practical issues arisen in HRES applications, including optimal design [10], scheduling and control [11, 12], maximum power point tracking (MPPT) [13], and economic analysis [14, 15].

In recent years, the HRES has been applied to hybrid-electric ships and all-electric ships [16]. On the one hand, new green ships are built with electric power systems, including PV, diesel generators (DGs), and battery [17, 18, 19]. On the other hand, existing fossil fuel

Nomenclature	
$P_1(t)$	power flow from diesel generator to internal bus (kW)
$P_2(t)$	power flow from internal bus to battery (kW)
$P_3(t)$	power flow from battery to internal bus (kW)
$P_4(t)$	bidirectional power flow between grid and internal bus (kW)
$P_{pv}(t)$	power output of PV panels (kW)
$P_{pl}(t)$	propulsion load of green ship (kW)
$P_{al}(t)$	auxiliary load of green ship (kW)
$P_D(t)$	power output of diesel generator (kW)
P_D^{max}	maximal power output of diesel generator (kW)
P_D^{max}	minimal power output of diesel generator (kW)
P_i^m	allowable maximal power on the ith line (kW)
v	status of switch on the grid connection
$\bar{v}$	inverse status of switch on the grid connection
$S(t)$	state of charge (SOC) of battery (%)
S^{max}	allowable maximum SOC (%)
S^{min}	allowable minimum SOC (%)
Q	capacity of battery (kWh)
η_C	charging efficiency of battery (%)
η_D	discharging efficiency of battery (%)
$\rho(t)$	price of electricity ($/kWh)

ships are undergoing energy efficient retrofit, and the HRES is installed to meet the axillary demand, such as loading, unloading, lighting, heating, cooling, and other on-board hotel services [20, 21]. Compared with the fossil-fuel ships, the hybrid-electric ships are less dependent on fossil fuel, and have more integration of solar or wind energy. The use of renewable energy can improve energy efficiency of ship, enhance reliability and quality of power supply, and reduce shipping cost and GHG emission. The hybrid power system on the green ship is usually regarded as a special case of mobile microgrid, which appears more complicated characteristics than the microgrid on land. System configurations are different when the ship is on voyage and berth, respectively. Environmental conditions are also extremely varying for the mobile microgrid. For the green ship, the mobile power system works on two modes, i.e., off-grid mode (stand-alone mode), and on-grid mode (grid-connected mode).

For the off-grid mode, many results have been reported in terms of optimal sizing [17, 18, 22], and power management [19, 21, 23]. In [17], an optimal sizing problem of stand-alone green ship has been formulated to minimize investment cost, fuel cost, and GHG emission, in which seasonal and geographical variation is considered for different routes. Interval optimization and clustering-based optimization methods have been proposed to determine the optimal size of energy storage system with uncertain PV power and load [18, 22].

To improve operational efficiency, power management has been studied for an electric ship with fuel cell, battery, PV panels, and diesel generators [19, 23]. For crane ships, lithium-ion batteries have been employed to take part into power management, in which a hybrid control strategy is developed to reduce fuel cost and GHG emission [21].

Other than the off-grid mode, green ships sometimes work on the grid-connected mode, when the shore-side grid power is available [20, 24]. As reported in [25], average harboring time of bulk carrier ship is about 2 months per year. As the shore-side power is usually cleaner than the power generated on board, the use of shore-side power, called cold ironing, can effectively reduce annual fuel cost and GHG emission, when the green ship is on berth. With the help of HRES, solar energy can be used to supply the on-board demand instead of the shore-side electricity, and electricity cost can be significantly reduced. In [20], a green cruise ship has been studied for delivering PV power to grid, and a rule-based strategy has been developed to satisfy auxiliary demand with batteries. In [24, 26], a unit commitment problem has been studied to optimally allocate power output of each diesel generator, in which cold ironing is considered.

Considering bidirectional power flow between green ship and shore-side grid, electricity tariffs must influence electricity cost of cold ironing, and possible reward from selling renewable energy to grid. Thus, the change

of electricity tariff will drive a different optimal solution to power management. To our best knowledge, very limited studies have evaluated tariff effects on power management of hybrid-electric ship. As a kind of demand side resources, on-grid green ships could take part into demand response programs, such as, time-of-use (TOU), and real time pricing tarrifs [27]. In this paper, the TOU tariff is studied as an instance of tariff-driven demand side management (DSM) of green ship. In the DSM, the HRES on a green ship can help owners to reduce electricity cost, and also can help utilities to enhance grid security and efficiency. Tariff-driven DSM of on-grid ship is more complicated than usual power management of off-grid ship, as demand-side management is required to consider the variance of electricity price and incentive reward, as well as the variance of renewable generation and load demand. One challenge of tariff-driven power management is to find an optimal control strategy for consuming grid power at the low-price period, and for selling renewable energy at the high-price period, while physical constraints have to be satisfied. Another challenge is to integrate the new capability of tariff-driven DSM into existing power management systems, which mainly focused on the off-grid management. The green ships often switch between on-grid and off-grid modes, especially for short-route ships, such as ferry and cruise. For this purpose, these challenging problems will be responded in the tariff-driven power management of green ship.

The contributions of this paper include three aspects. Firstly, tariff effects are studied for the power management of green ship with HRES, which is formulated as an optimal power dispatching problem to minimize the operational cost. Secondly, a unified tariff-driven power management system for off-grid and on-grid modes is proposed to optimally schedule the ship all the time. Thirdly, receding horizon control is proposed in the green ship application, so that system disturbances on solar energy and load demand can be detected and corrected. The resulted performance is promising with respect to energy efficiency and robustness. This paper is organized as follows. A HRES is introduced for the green ship in Section 2. Optimal power management problem of off-grid green ship is formulated in Section 3. A tariff-driven power management model is proposed in Section 4. Receding horizon control is proposed to control power flows for the minimization of operational cost in Section 5. Results and discussions are presented in Section 6, while the last section is the conclusion.

2. Hybrid renewable energy system of green ship

PV-DG-battery (PDB) hybrid systems are successfully applied to green ships [19, 23]. The PDB system is made up of three main subsystems, i.e., PV panels, battery storage, and DG. The ship load includes propulsion load and auxiliary load. Auxiliary load consists of lights, water heating, air conditioners, plug-in devices, and other on-board hotel facilities. For the PDB hybrid system of green ship, the basic requirement is to keep the power balance, and to reduce operational cost and GHG emission.

Regarding to different volume and rated power, the hybrid electric ship can be categorized into two types. The first kind of ships, such as, bulk cargo vessels, which has large volume and rated power, only depends on DGs for the propulsion power. The solar energy is used to meet the hotel and auxiliary load, as shown in Figure 1(a). The second kinds of ships, such as, cruises and ferries, usually have small volume and rated power. Both DG and solar energy are integrated to supply power for the propulsion load and auxiliary load, as shown in Figure 1(b).

In this paper, we study the power management of a retrofitted green ship, which belongs to the first type, as shown in Figure 1(a). The propulsion load is directly supplied by the DG. For the auxiliary load, the PV power has the first priority of usage, and the battery takes part in the power supply when the PV output is not enough to meet the auxiliary load. Only when both PV and battery cannot meet the ship load, the DG eventually comes in due to its highest cost.

Note that there is an internal bus in the hybrid electric ship, as shown in Figure 1. The shore-side grid can be connected with the ship internal bus for the cold ironing. The propulsion load is denoted as P_{pl}, and the auxiliary load is denoted as P_{al}. The power flows from the DG, battery and PV to the bus are denoted as P_1, P_3 and P_{pv}, respectively. P_2 represents the power flow from the bus to battery. The subsystems, i.e., PV, DG, and battery, are introduced as follows.

2.1. PV panel

A solar panel usually consists of several solar cells to convert solar irradiation into direct current power. In the application of green ship, the PV panels installed in different parts of ship can be categorized as different groups, e.g., the PV panels installed on the top deck, the lower deck, the vertical surface, and some discontinuous space. These groups may have different irradiance and shading characteristics during the long-term voyage. The power output of each PV panel can be simply
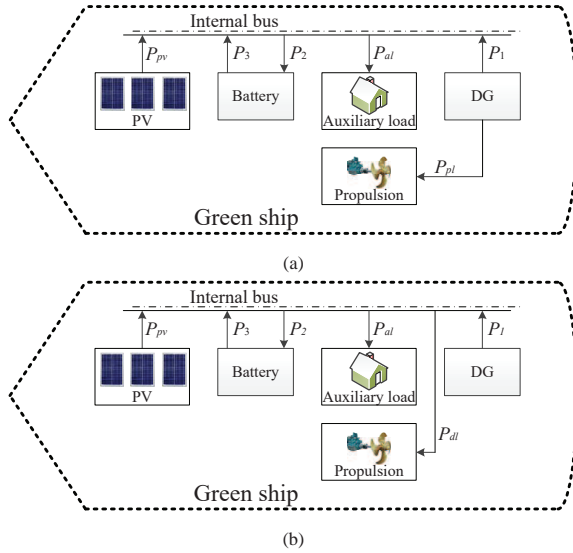
Figure 1: Schematic of the off-grid PDB hybrid system on green ships: (a) DG propulsion; (b) electric propulsion.

formulated as:

$$P_{pv}(t) = \eta_{pv} I_{pv}(t) A_c, \qquad (1)$$

where t is the time of day; P_{pv} is the power output from the PV panel; η_{pv} is the efficiency of solar generation; I_{pv} is the solar irradiation incident on the PV panel; A_c is the size of PV panel.

The hourly solar irradiation incident on the PV panel has complicated relations with time of a day, season of a year, tilt, location, global irradiation, and diffuse fraction. In this study, the simplified isotropic diffuse formula is used according to [28, 29]. The solar irradiation incident can be expressed as

$$I_{pv}(t) = [I_B(t) + I_D(t)]R_B(t) + I_D(t), \qquad (2)$$

where I_B is the beam component of global irradiation, and I_D is diffuse irradiation. R_B is a geometric ratio of actual irradiation on the tilted plane to the standard irradiation on the horizontal plane.

The efficiency of solar generation can be expressed as a function of the irradiation I_{pv} and the ambient temperature T_A as

$$\eta_{pv} = \eta_R \left[1 - \frac{0.9 \beta I_{pv}(T_{C0} - T_{A0})}{I_{pv0}} - \beta(T_A - T_R) \right], \qquad (3)$$

where η_R is the PV generation efficiency that is measured at the referenced cell temperature T_R (25°C); β is

the temperature coefficient for cell efficiency (typically 0.004-0.005 /°C); T_{C0} (typically 45°C) and T_{A0} (typically 20°C) are cell temperature and ambient temperature at the nominal operating cell temperature (NOCT) test, respectively; I_{pv0} is the average solar irradiation on the array at the NOCT test.

2.2. Diesel generator

Diesel generators are commonly used as engines in green ships. They are also incorporated in the PDB hybrid system to supply the auxiliary demand, when solar power and battery storage are insufficient. It is a common sense that the fuel consumption is determined by the power output. This relation is usually expressed as a quadratic model [24, 26]. The fuel consumption can be formulated as

$$\mu_{DG}(t) = d_1 P_D(t)^2 + d_2 P_D(t) + d_3, \qquad (4)$$

where μ_{DG} is diesel consumption rate (the volume of diesel consumed per hour); $P_D(t)$ is the power output of DG; d_1, d_2, and d_3 are generation coefficients. When the power output is large, the DG efficiency is large (the fuel cost per kWh is small). According to Eq. (4), the hourly fuel cost can be calculated. DG's power output has to be restricted between the rated power and specified minimum value as

$$P_D^{min} \leq P_D(t) \leq P_D^{max}, \qquad (5)$$

where P_D^{max} is the rated power and P_D^{min} is the minimum requirement of power output.

2.3. Battery bank

Many kinds of battery, such as Lead-acid, Nickel-based, and Lithium-ion cells, have been used in the PDB hybrid system. In general, the battery storage is closely related with maximum capacity and state of charge (SOC). Note that SOC is defined as the percent of remained storage.

The SOC could change dynamically due to possible charge or discharge. Let $S(t)$ denote the SOC of battery at time t, and $S(0)$ denote the original SOC. The change of SOC can be formulated as

$$QS(t) - QS(0) = \eta_C \int_{\tau=0}^{t} P_2(\tau) d\tau - \frac{1}{\eta_D} \int_{\tau=0}^{t} P_3(\tau) d\tau, \qquad (6)$$

where Q is the maximum capacity of battery; $P_2(t)$ is the power for charging the battery at time t; $P_3(t)$ is the power of discharge at time t. The first component at the right-hand side means the total energy stored to the battery, and the second component means the total

energy consumed. $\eta_C \leq 1$ and $\eta_D \leq 1$ are charging efficiency and discharging efficiency [9, 30]. The charging/discharging loss comes from the heat loss of cells and converters.

By the differentiation at both sides of Eq. (6), the dynamics of SOC can be expressed as

$$\dot{S}(t) = \frac{\eta_C}{Q} P_2(t) - \frac{1}{Q\eta_D} P_3(t). \qquad (7)$$

The battery has strict constraints on the upper and lower bounds of SOC. The upper bound is defined as S^{max}, and the lower bound is defined as S^{min} in this paper. The SOC must be bounded within the scale $[S^{min}, S^{max}]$.

3. Power management of off-grid mode

For the voyaging ship, how to minimize the fuel consumption for each day is a critical issue of power management, which is referred to power flow dispatching. Optimal dispatching will be studied to determine daily schedule of PDB hybrid system for minimizing the fuel cost. The daily fuel cost is formulated as

$$C_1 = p \sum_{k=0}^{N-1} [d_1 P_D^2(k) + d_2 P_D(k) + d_3], \qquad (8)$$

where N denotes the evaluation period. The sampling period is an hour for instant, so $N = 24$ for a day. Note that the sampling period can be determined by users. C_1 is the fuel cost over the evaluation period; p is the fuel price. $P_D(k)$ is the diesel's power output over the period [k,k+1), which can be expressed as

$$P_D(k) = P_{pl}(k) + P_1(k), \qquad (9)$$

where $P_{pl}(k)$ is the propulsion load over [k,k+1).

Furthermore, each component of PDB hybrid system suffers from continuous wearing over the rated lifetime [4]. According to [8, 31], the daily wearing cost of system can be simplified as

$$C_2 = \tau_1 \sum_{k=0}^{N-1} [P_2(k) + P_3(k)] + N\tau_2, \qquad (10)$$

where the first component is the wearing cost of battery, and the second component is the wearing cost of other subsystems, such as DG and solar panel. τ_1 is the coefficient of battery wearing, and τ_2 is the hourly wearing cost of other components. ($\tau_1 = 0.001$ and $\tau_2 = 0.002$ in the studied system.) Note that the first component

can indicate the amount of charging/discharging cycle, as the battery usually works in full cycles due to SOC boundary. In the second component, we assume the constant wearing cost, as the wearing rate rarely changes for a given transportation task, e.g., the fixed propulsion load and the fixed frequency of start/stop.

Considering fuel cost and wearing cost, the objective of optimal power flow dispatching is to minimize off-grid operational cost J_f as

$$J_f = C_1 + C_2. \qquad (11)$$

For the application of green ship, several physical and operational constraints have to be satisfied.

(1) Power balance constraint: The PV power, battery power, and possible DG power output must exactly match the auxiliary demand P_{al}. Power imbalance may harm all electric components in the PDB system. The power balance can be formulated as

$$P_1(k) + P_3(k) + P_{pv}(k) = P_2(k) + P_{al}(k). \qquad (12)$$

(2) DG output constraint: The DG power output must be less than the rated power and larger than the specified minimum.

$$P_D^{min} \leq P_{pl}(k) + P_1(k) \leq P_D^{max}. \qquad (13)$$

(3) Power flow constraint: For safety and other physical reasons, power flow on each line must be bounded by a maximum value as

$$0 \leq P_i(k) \leq P_i^m, i = 1, 2, 3, \qquad (14)$$

where P_i^m is the allowable maximum power delivered on the ith line.

(4) SOC boundary constraint: During charging or discharging, SOC has the upper and lower bound for ensuring state of health.

$$S^{min} \leq S(k) \leq S^{max}. \qquad (15)$$

(5) SOC terminal state constraint: For the convenience of daily dispatching power, the terminal SOC of battery must be no less than the initial SOC as

$$S(0) \leq S(N). \qquad (16)$$

For the off-grid mode, the power flow dispatching problem is modeled as a standard quadratic programming problem with equality and inequality constraints. In this optimization model, the objective function is (11), and the constraints include (12-16). The control variables are $P_1(k)$, $P_2(k)$, and $P_3(k)$ for each hour. Like

other off-grid power flow dispatching models [24, 26], PV output and auxiliary load are assumed known as priory knowledge in this study. Short-term deviations can be taken over by the ship real time control system through certain adjustment mechanisms [26]. In a day, load demand and PV power are series of data indexed by time, which can be forecasted based on historical data. Time series analysis models, including autoregressive (AR) [32] and neural networks [33, 34, 35], have been studied for short-term and long-term forecast of future PV and load profiles. Note that electricity tariffs have no effects on power management for the off-grid mode.

4. Tariff-driven power management

When the green ship has stopped in the harbor for loading, unloading, or maintenance, the propulsion load is zero, and the green ship has the grid connection. Electricity tariffs at harbor have great effects on the solution to power management. For this on-grid mode, power management requires a tariff-driven power dispatching method, and the off-grid dispatching method is not able to suit the on-grid mode. The structure of on-grid green ship is given in Figure 2. In this paper, the TOU tariff is considered as a typical incentive policy for studying the tariff-driven power management.
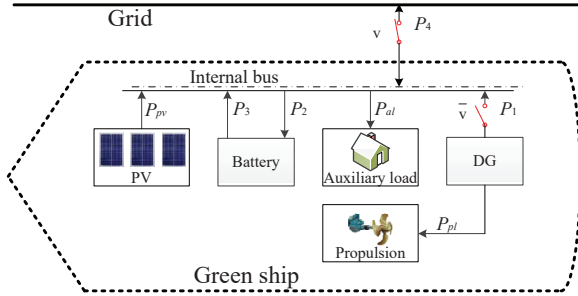

Figure 2: A unified structure of green ship

In the TOU tariff, electricity price changes over different periods according to the imbalance situation between power supply and demand. For example, a high price is paid for the peak load period; a medium price is paid for the standard period; and a low price is paid for the off-peak period. In this study, electricity price at the target harbor is

$$\rho(t) = \begin{cases} \rho_k, & t \in T_k, \\ \rho_o, & t \in T_o, \\ \rho_s, & t \in T_s, \end{cases} \tag{17}$$

where ρ_k is the price of peak load period T_k; ρ_o is the price of off-peak period T_k; ρ_s is the price of standard period T_s.

Let P_4 denote the bi-directional power flow between the grid and green ship. Define $P_4 > 0$ when the grid power flows to the ship, and $P_4 < 0$ when the ship supplies power to grid. It can be noticed that the role of ship, as load or distributed generation, determines the sign of P_4. For safety, the bi-direction power flow has to be bounded as

$$-P_4^m \le P_4(k) \le P_4^m, \tag{18}$$

where P_4^m is the allowable maximum of power flow on this connection.

The daily cash flow, associated with buying and selling electricity, can be formulated as

$$C_3 = \sum_{k=0}^{N-1} \rho(k)P_4(k), \tag{19}$$

where C_3 represents the daily cash flow driven by the TOU tariff. Note that $C_3 > 0$ means cash-out, i.e., electricity cost. $C_3 < 0$ means cash-in, i.e., electricity reward. For the on-grid situation, the minimization of daily cash flow is expected in the tariff-driven power management.

The capability of tariff-driven dispatching will be integrated in the existing power management system. In this paper, a unified dispatching model will be studied to handle both off-grid and on-grid modes in an automatic manner. For the unified model, power flow dispatching has to consider the optimization of fuel cost, wearing cost, and possible electricity cost caused. The optimization problem is closely related with the status of switch. Based on the on/off status, the objective function can be expressed as

$$J_u = C_1 + C_2 + vC_3. \tag{20}$$

where J_u is the daily cost of the unified model. v is the status of switch. $v = 0$ means off-grid mode, and $v = 1$ means on-grid mode. C_1 is the fuel cost expressed as Eq. (8); C_2 is the wearing cost expressed as Eq. (10); C_3 is the electricity cost expressed as Eq. (19). If $v = 1$, grid connection is introduced, and tariff-driven power management is enabled.

Based on the status of switch, constraints, e.g., power

balance and boundary, also have to be re-formulated as

$$\begin{cases} P_1(k) + P_3(k) + vP_4(k) + P_{pv}(k) = P_2(k) + P_{al}(k), \\ (1-v)P_D^{min} \le (1-v)P_{pl}(k) + P_1(k) \le (1-v)P_D^{max}, \\ 0 \le P_1(k) \le P_1^{max}, \\ 0 \le P_2(k) \le P_2^{max}, \\ 0 \le P_3(k) \le P_3^{max}, \\ -P_4^m \le vP_4(k) \le P_4^m, \\ S^{min} \le S(k) \le S^{max}, \\ S(0) \le S(N), \end{cases}$$

(21)

For the unified model, three main characteristics are essential. Firstly, when the switch is off, the model must be equivalent with the proposed off-grid dispatching model. The optimal solution ensures minimal fuel cost and wearing cost during the voyage. Secondly, when the switch is on, the surplus of PV power can be sold to grid, and the hybrid system serves as a role of distributed generation. This could help release the peaking burden of grid, and earn possible incentive reward that depends on the policy of harbor. Thirdly, for taking advantage of incentive policies, battery can store the grid power at the off-peak time, and can be discharged during the peak time.

As a result, the unified model successfully covers off-grid and on-grid modes. In Figure 2, two modes are changed by a switch V. The green ship is on-grid if the switch V is on (i.e., $v = 1, \overline{v} = 0$). If V is off (i.e., $v = 0, \overline{v} = 1$), the green ship is off-grid. For the off-grid situation, the system structure is the same as Figure 1(a). In a unified model, the status of V is a variable detected in real time, and then the optimization of power flow is re-conducted periodically. If $v = 0$, it is obvious that the unified model is equivalent with the off-grid model studied in the previous section. If $v = 1$, the unified model can reflect all essential characteristics of the on-grid mode.

5. Receding horizon control

Based on current status, optimal schedule over next 24 hours can be obtained via the optimization of the unified model. However, the status of switch and the SOC of battery could change over next 24 hours due to uncertain solar generation and traveling time. This happens when the green ship is about to approach the harbor or to leave. Then, the original scheduling results cannot be used to control the PDB hybrid system. For this purpose, receding horizon control is proposed based on periodic optimization, as shown in Figure 3

In the proposed receding horizon control, the optimization proceeds iteratively to utilize the real-time
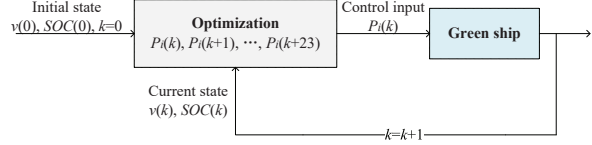

Figure 3: Illustration of receding horizon control

feedback information, i.e., the SOC and the status of switch. For each time, only the first component of optimal solution is employed to control the hybrid system. For example, a voyaging green ship will arrive at the harbor and connect to grid after 20 hours. After detection of current state, the unified optimization model is an off-grid model, and the daily schedule of off-grid ship can be obtained by the optimization over the prediction horizon, i.e., 24 hours. The first component of optimal solution is the power flow for the 1st hour, which is employed as the control input. The SOC may be changed due to possible charging or discharging. After 1 hour, the switch is still off, and the same procedure is repeated, until the green ship is connected to grid. After 20 hours, the status of switch is on. The unified optimization model is an on-grid model, and optimal dispatching can be obtained by the optimization of operational cost. The first component of optimal solution is the power flows for the 21th hour. This procedure is repeated till any stopping criterion is satisfied.

The procedure of receding horizon control for the green ship has been given in Algorithm 1. An optimization problem over the prediction horizon is repeatedly solved ($k = 0, 1, \ldots$). The optimization variable is the power flows over the following N intervals. At the kth sample, based on current states detected, an optimal solution denoted as $[\tilde{P}_l(k|k), \tilde{P}_l(k+1|k), \ldots, \tilde{P}_l(k+N-1|k)]^T$ can be obtained. Only the first component of solution, i.e., $\tilde{P}_l(k|k)$, is used as the control input over $[k, k+1)$. Note that the receding horizon control has the mechanisms of feedback and real-time control.

Receding horizon control is also called model predictive control (MPC) [36, 37]. The key concept of receding horizon control is that control variables are calculated by using the optimization approach, but only the first component is taken as the control input at the current stage. As the optimization is conducted based on the current observation of state variables, state feedback is inherently incorporated in the receding horizon control. For the next interval, the prediction over the receding horizon is recalculated. As the close-loop control is implemented based on real-time updated information, the disturbance can be detected and corrected in the pro-

```
1 Set k = 0;
2 while the stopping criterion is not satisfied do
3 │  Detect the SOC and the status of switch;
4 │  Minimize the objective function (20) subject to
  │  constraint (21);
5 │  For the optimal solution, apply P̃ᵢ(k|k) to the
  │  system at the period [k, k + 1);
6 │  k = k + 1;
7 end
```

Algorithm 1: Pseudo-code of the receding horizon control approach

posed approach.

In the receding horizon control, each optimization problem is a quadratic programming problem. Let $u(k) = [P_1(k), P_2(k), P_3(k), P_4(k)]$ denote the control inputs. Then the minimization of function (20) can be converted into a standard form of quadratic programming as

$$\min \frac{1}{2}(U^T * H * U + f * U), \qquad (22)$$

where $U = [u(k), u(k+1), ..., u(k+N-1)]^T$. H and f are parameters that can be deduced according to (20).

For power flow dispatching, there are mainly two types of methods, i.e., ruled based and optimization-based methods. The proposed receding horizon control is an optimization-based method. For the purpose of comparison, a rule-based control is referred to fulfilling the satisfaction of constraints. In the rule-base control, the solar power has the highest priority of usage. The solar power is employed for satisfying the load demand or charging the battery. If the load demand cannot be satisfied by the solar power, the battery power is used. If the batter is over-discharged, the grid power or diesel is then integrated. For time t, the control input is decided as the following steps:
(1) If $P_{al}(t) \leq P_{pv}(t)$, $P_1(t) = 0$ and $P_3(t) = 0$. In this case, $P_2(t) = P_{pv}(t) - P_{al}(t)$ and $P_4(t) = 0$ if $S(t) < S^{max}$; otherwise $P_2(t) = 0$ and $P_4(t) = P_{pv}(t) - P_{al}(t)$.
(2) If $P_{al}(t) > P_{pv}(t)$ and $S(t) > 0.7S^{max}$, then $P_1(t) = 0$, $P_2(t) = 0$, $P_3(t) = P_{al} - P_{pv}(t)$, and $P_4(t) = 0$.
(3) If $P_{al}(t) > P_{pv}(t)$ and $S^{min} < S(t) \leq 0.7S^{max}$, then $P_2(t) = 0$, and $P_3(t) = 0$. In this case, $P_1(t) = 0$ and $P_4(t) = P_{al} - P_{pv}(t)$ if $v(t) = 1$, otherwise $P_1(t) = P_{al} - P_{pv}(t)$ and $P_4(t) = 0$.
(4) If $P_{al}(t) > P_{pv}(t)$ and $S(t) < S^{min}$, then $P_2(t) = S^{min} - S(t)$, and $P_3(t) = 0$. In this case, $P_1(t) = 0$ and $P_4(t) = P_{al} - P_{pv}(t) + P_2(t)$ if $v(t) = 1$, otherwise $P_1(t) = P_{al} - P_{pv}(t) + P_2(t)$ and $P_4(t) = 0$.

6. Results and discussions

6.1. Experimental results

A certain hybrid electric green ship with maximum power 500 kW is evaluated in this section. Note that the studied ship has been properly designed for matching its rated volume and power. Some advanced methods, such as optimal sizing and economic analysis [10, 17, 38], can be considered at the design stage of new green ships. As the scope of this paper is the power management for scheduling the operation of green ship, the issues on system design are excluded in this study.

Voyage tests at the ocean area of South Africa, are reported in the paper. Note the voyage schedule is calculated via other motion planning methods, while traveling constraints must be satisfied in the resulted voyage schedule. For the given route, the operational cost of ship will be evaluated under different seasons (summer vs. winter) and weather (sunny vs. cloudy). The structure of PDB hybrid system is the same as Figure 2. In the application, the PV panels are installed in different parts of the ship, i.e., top deck, lower deck, vertical surface, and other discontinuous space. For the PDB hybrid system, configurations are mainly introduced here.

The storage bank consists of 272 Lithium-ion batteries. 4 batteries are serially connected as a set, and 68 sets, connected in parallel, form the bank. For each battery, the voltage is 12 V, and the capacity is 150 Ah. Therefore, the nominal capacity of storage bank is 489.6 kWh. The PV module consists of 240 PV panels, each of which has the capacity 250 W, so the rated PV output is 60 kW. The maximal power point tracking is integrated in each PV adapter. AC/DC and DC/AC inverters are also employed for each line. The parameters of this system are listed in Table 1. Note that charging and discharging efficiency are regarded as 85% and 95% in this paper for the target system. During the lifetime, energy efficiency may decrease due to system performance deterioration. This factor of efficiency decrease will be evaluated in the discussion part.

For regular cruising, the propulsion load is 100 kW. For berthing, the propulsion load is 0 kW. the daily profiles of auxiliary load and PV power are regarded as the average values over the past week before the test day (July 28, 2017, Cape Town), as shown in Figure 4. Given known profiles of auxiliary load and PV output, optimal power dispatching can be obtained in the proposed control approach. Note that actual profiles of the test day could have small differences with the average profiles, differences will be corrected in the proposed receding horizon control, as evaluated in the discussion part.

8

Table 1: Parameters of PV-battery system

|	
Nominal battery capacity	489.6 kWh
Battery charging efficiency	85 %
Battery discharging efficiency	95 %
Initial SOC	60 %
Minimum of SOC	40 %
Maximum of SOC	100 %
PV array's capacity	60 kW
fuel price	0.67 \$/L
Rated power of diesel	500 kW
Regular cruising propulsion load	100 kW
Minimal output of diesel	5 kW
d_1	0.000036
d_2	0.1728
d_3	76.8
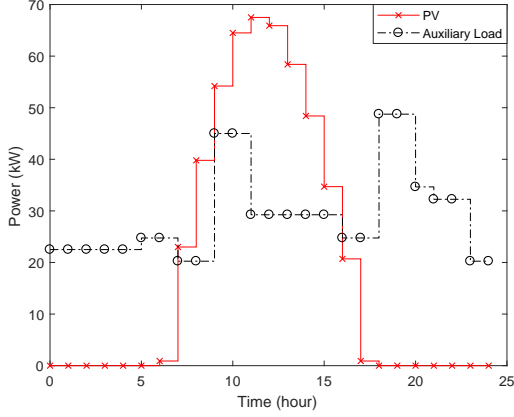
Figure 4: Daily profiles of auxiliary load and solar energy in the test

Remark 1: Although solar irradiation mainly depends on time of day, it changes intensively under different environment, such as, location, season, orientation, and weather. For specific environmental conditions, daily profiles of overall PV generation on the ship show certain periodical characteristics. Advanced prediction methods can ensure promising accuracy, when environment change is trivial.

Remark 2: In some simple operating situations, ship load and PV output are fixed and known. For example, propulsion and axillary load is the same as historical days. The proposed model can deliver stable performance of minimal fuel cost and GHG emission. For complicated situations, the propulsion load is determined by the mass of ship and cargo, and auxiliary load is time-varying due to human behavior and external en-

vironment. Thus, system identification methods, such as model-based and data-driven methods, are required to determine propulsion and auxiliary load.

As the focus of this paper is system model and receding horizon control, the profiles of auxiliary load and PV power are regarded as the average historical values for simplicity. More advanced forecast methods [24, 26, 32, 39] can be utilized as preliminary steps of the proposed approach.
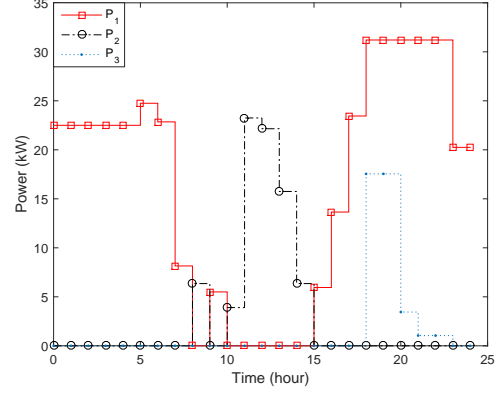
(a)
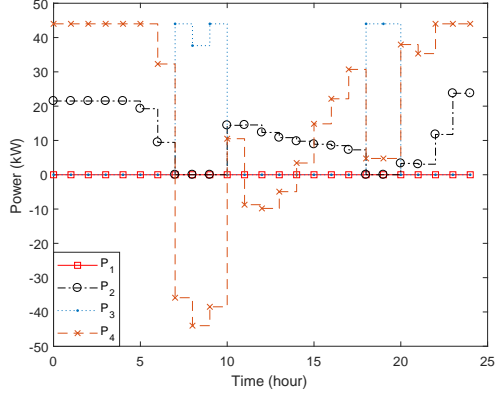
(b)

Figure 5: Power flows of green ship in 24 hours: (a) off-grid; (b) on-grid

For the 24-hour and 3-day tests, the TOU tariff (denoted as TOU-1) is

$$\rho_1(t) = \begin{cases} 0.157, & t \in [7,10) \bigcup [18,20), \\ 0.077, & t \in [0,6) \bigcup [22,24), \\ 0.113, & t \in [6,7) \bigcup [10,18) \bigcup [20,22), \end{cases}$$

(23)

(1) *24-hour test*

The 24-hour test is conducted for both off-grid and on-grid modes. For each mode, optimal power flows obtained in the receding horizon control are plotted in Figure 5. For the off-grid mode, the DG is the main power supplier. Battery is discharged at midnight, and is charged when the solar irradiation is sufficient at noon. For the on-grid mode, the grid is the main power supplier. However, battery is charged at midnight due to low electricity price, and discharged for selling electricity at the peak period. Although the DG power sometime decreases, i.e., the DG turns less efficient, energy efficiency of the whole system is improved. The reason is that the reduction of DG power is taken place by the cheap PV power or battery power.

The daily cost, including fuel cost and wearing cost, is evaluated. Without the integration of hybrid system, the daily cost is \$1604.2. In the rule-based control, the daily cost is \$1571.3. In the receding horizon control, the daily cost can be reduced to \$1566.9. If the green ship is stopping in port with the grid connection, the daily cost includes electricity cost and wearing cost. Without the integration of hybrid system, the daily cost is \$81.0. In the rule-based control, the daily cost is \$47.2. In the receding horizon control, the daily cost can be reduced to \$29.0. It can be noticed that the integration of hybrid system can effectively reduce the expense of ship, and the receding horizon control can achieve the minimal cost.

(2) *3-day test*

The 3-day test is conducted to verify the power management for complicated situations. The change of off-grid and on-grid modes will be evaluated in a 3-day route. The green ship is off-grid at 0am of the first day, and gets the grid connection since 8pm of the first day.

Based on the unified model, results of power flow and SOC are plotted in Figure 6. Before the arriving time, the results of receding horizon control are similar with those of the 24h off-grid experiment. The main power supplier is the DG, and the battery is charged at noon. In contrast, the results after arrival are similar with the 24h on-grid experiment. The main power supplier turns to be the grid, and the battery is charged at midnight.

The overall cost over 3 days will be evaluated. Without the integration of hybrid system, the overall cost is \$1519.7. With the help of hybrid system, the daily cost is \$1392.5, and the SOC is 71.5% for the rule-based control. For the receding horizon control, the overall cost is \$1368.4, and the SOC is 65%. The difference of residual energy in the bank, worth about \$3, can be negligible. It is obvious that receding horizon control can result in an optimal strategy with the minimal cost.

It can be concluded that the unified model can effec-
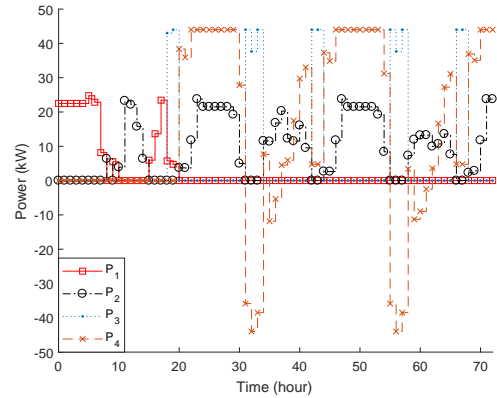
(a)
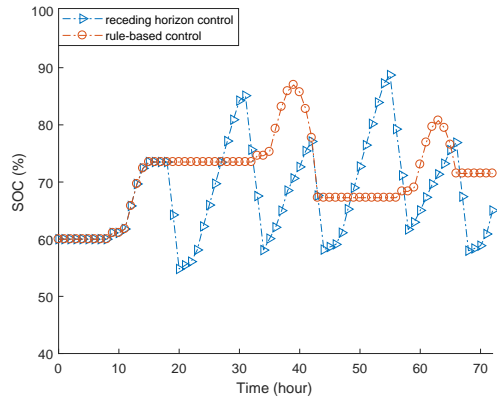
(b)

Figure 6: Experimental results of green ship in 3 days: (a) power flows of receding horizon control; (b) SOC profiles

tively handle two different modes, and that the overall cost can be minimized by the receding horizon control regardless to the change of mode. If the harboring period is 2 months per year, the operational cost of green ship can be reduced by about \$14300 per year. Compared with fuel ships without PV generation, fuel consumption and GHG emission of green ship can be reduced by about 3% for each year.

6.2. Discussions

The aforementioned results are reported based on tests during sunny winter days. However, the environmental change must influence the solar energy on the green ship, and the operational cost as well. Firstly, environmental effects on the green ship will be discussed in this part. Secondly, charging and discharging efficiency must change month by month due to system de-

terioration. Effects of varying parameters on the green ship will also be discussed. Thirdly, effects of forecast error are discussed, as it has influenced the control performance. At last, effects of different TOU tariffs are evaluated in the tariff-driven approach.

(1) *Effects of environmental conditions*

The green ship is tested on 4 kinds of environment, i.e., a sunny winter day(July 28, 2017, Cape Town), a cloudy winter day (August 3, 2017, Cape town), a sunny summer day (Jan 29, 2017, Cape Town), and a cloudy summer day (Feb 18, 2017, Cape Town). Different environmental conditions mainly influence daily profiles of PV power. Other parameters are assumed the same as listed in Table 1.

The daily cost under different environment is listed in Table 2. For a sunny summer day, solar energy generation is the largest, so the green ship has the smallest operational cost for each mode. For a cloudy winter day, solar energy generation decreases the most, so the operational cost is the largest. In the same season, solar generation on a sunny day is larger than a cloudy day, so the operational cost on a sunny day is smaller than a cloudy day. In the comparison of summer and winter, daily solar generation in summer is larger than winter, so the daily cost in summer is usually smaller than winter for the sunny and cloudy weather, respectively.

(2) *Effects of charging and discharging efficiency*

To test effects of charging efficiency, the charging efficiency is set as 95%, 85%, 75%, 65%, and 55%, respectively. The other settings are kept the same as listed in Table 1. Note that the initial SOC is 60% and the discharging efficiency is 95%.

For the receding horizon control, the daily cost under different charging efficiency is listed in Table 3. It can be observed that high charging efficiency is preferred to reduce the daily cost. When the battery gets old with low charging efficiency, the daily cost will increase. Especially for the on-grid ship, more reward can be earned when the charging efficiency is larger. It is suggested to retrofit a new battery when the charging efficiency is lower than 70%.

To test the discharging efficiency, the discharging efficiency is set as 95%, 85%, 75%, 65% and 55% respectively. The other settings are kept the same as listed in Table 1. Note that the initial SOC is 60% and the charging efficiency is 85%.

The daily cost under different discharging efficiency is given in Table 4. Effects of discharging efficiency are similar with those of charging efficiency. The cost increases, as the battery has relatively low discharging efficiency. A new battery is suggested for retrofitting when the discharging efficiency is lower than 80%.
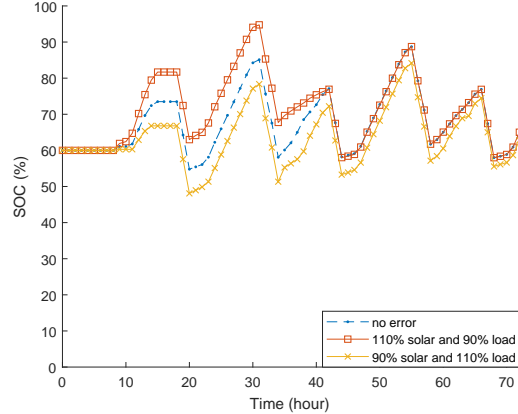

Figure 7: SOC's sensitivity on forecast errors

(3) *Effects of forecast error*

To test effects of forecast error, the actual load demand is assumed as 90% of the forecast of load, and the actual solar power is assumed as 110% of the forecast of solar power at the first day. There is no forecast error in the next two days in this test. The SOC sensitivity on uncertain forecast errors is analyzed as shown in Figure 7. When no forecast error exists, the SOC profile is a baseline for the sensitivity analysis. It can be observed that forecast errors of load and solar cause variance of SOC. More power is stored in the battery when the system has less load and more solar power than the predicted values. The SOC profiles keep close and converge in finite time, which can indicate the proposed receding horizon control has good robustness when the forecast errors exist.

In comparison, the actual load demand is also assumed as 110% of the load forecast, and the actual solar power is assumed as 110% of the forecast. When the load demand is 90% and the PV power is 110%, the electricity cost decreases to $1356.1, because more solar power is stored in the battery and less grid power is consumed. When the load demand is 110% and the PV power is 90%, the electricity cost increases to $1379.3, because the actual load demand is larger than the forecast value. Note that the electricity cost is $1368.4 if forecast error is zero.

(4) *Effects of tariff change* To test effects of different tariff, another TOU tariff (denoted as TOU-2) is considered as

$$\rho_2(t) = \begin{cases} 0.132, & t \in [11,17), \\ 0.065, & t \in [19,24) \cup [0,7), \quad (24) \\ 0.095, & t \in [7,11) \cup [17,19), \end{cases}$$

Table 2: Daily cost under different environment

	Cloudy winter	Sunny winter	Cloudy summer	Sunny summer
off-grid cost($)	1589.4	1566.9	1581.4	1557.9
on-grid cost ($)	55.63	29	47.37	13.05

Table 3: Daily cost under different charging efficiencies

η_C	95%	85%	75%	65%	55%
off-grid cost($)	1562.8	1563.7	1564.6	1565.5	1566.4
on-grid cost ($)	25.87	29.04	32.67	35.08	37.48

Table 4: Daily cost under different discharging efficiencies

η_D	95%	85%	75%	65%	55%
off-grid cost ($)	1563.7	1564.5	1565.3	1566.1	1566.9
on-grid cost ($)	29.04	32.42	34.57	36.72	38.15

For the 24-hour test of on-grid mode, the daily cost under TOU-1 tariff is $29, but the daily cost under TOU-2 tariff is $-125.4. In other words, the hybrid electric system can earn $125.4 under TOU-2 tariff. Figure 8 shows the optimal solution to power dispatching. Comparing Figure 5(b) and Figure 8, it can be observed that the optimal solutions under different TOU tariffs are also different, as peak/off-peak period and electricity price changes.

Figure 8: Optimal power dispatching under the TOU-2 tariff

7. Conclusion

Considering effects of different tariff, power management of green ship, with the PDB hybrid system, is studied in the receding horizon control approach. Both the stand-alone and grid-connected modes are considered in a unified power flow dispatching model. The receding horizon control is proposed to iteratively optimize operational cost, including possible fuel cost, wearing cost, and electricity cost. Regardless of variant environmental conditions, optimal dispatching strategies of green ship can be obtained to reduce fuel consumption and GHG emission by about 3% per year.

Experimental results have indicated several conclusive points. Firstly, the green ship is an effective resource to join in demand side management. Under TOU tariffs, optimal power management of green ship can contribute energy efficiency improvement on shipping industry and electricity market. Secondly, the capability of tariff-driven dispatching is successful integrated in the unified model of power management. Two working modes, i.e., off-grid management and on-grid management, can be handled in an automatic way. Thirdly, receding horizon control is a robust approach to power management of green ship. With the feedback mechanism, forecast errors and other disturbance have been detected and corrected in the control, and the performance of energy efficiency and cost saving is lasting.

The green ship studied in this paper is a retrofitted ship with hybrid electrification. The proposed model can be extended to all-electric green ships as future work. Multiple generation resources, such as different kinds of distributed energy and energy storage systems, will be studied in the green ship in future.

8. Acknowledgement

ties, 106112016CDJRC000014, and 106112017CD-JXY170003.

References

[1] Buhaug Ø, Corbett J, Endresen Ø, Eyring V, Faber J, Hanayama S, et al. Second IMO CGC study 2009. London, UK: International Maritime Organization (IMO); 2009,.

[2] Diab F, Lan H, Ali S. Novel comparison study between the hybrid renewable energy systems on land and on ship. Renewable and Sustainable Energy Reviews 2016;63:452 –63.

[3] Tazvinga H, Xia X, Zhang J. Minimum cost solution to photovoltaic-diesel-battery hybrid power systems for remote consumers. Solar Energy 2013;96:292 –9.

[4] Tazvinga H, Zhu B, Xia X. Optimal power flow management for distributed energy resources with batteries. Energy Conversion and Management 2015;102:104 –10.

[5] Nema P, Nema R, Rangnekar S. A current and future state of art development of hybrid energy system using wind and PV-solar: A review. Renewable and Sustainable Energy Reviews 2009;13(8):2096 –103.

[6] Shaahid S, El-Amin I. Techno-economic evaluation of off-grid hybrid photovoltaic-diesel-battery power systems for rural electrification in saudi arabia — a way forward for sustainable development. Renewable and Sustainable Energy Reviews 2009;13(3):625 –33.

[7] Palma-Behnke R, Benavides C, Lana F, Severino B, Reyes L, Llanos J, et al. A microgrid energy management system based on the rolling horizon strategy. IEEE Trans on Smart Grid 2013;4(2):996 – 1006.

[8] Wu Z, Tazvinga H, Xia X. Demand side management of photovoltaic-battery hybrid system. Applied Energy 2015;148:294 – 304.

[9] Wu Z, Xia X. Optimal switching renewable energy system for demand side management. Solar Energy 2015;114(0):278 –88.

[10] Arun P, Banerjee R, Bandyopadhyay S. Optimum sizing of photovoltaic battery systems incorporating uncertainty through design space approach. Solar Energy 2009;83(7):1013 –25.

[11] Gabash A, Li P. Flexible optimal operation of battery storage systems for energy supply networks. IEEE Trans on Power Systems 2013;28(3):2788 –97.

[12] Kanchev H, Lu D, Colas F, Lazarov V, Francois B. Energy management and operational planning of a microgrid with a PV-based active generator for smart grid applications. IEEE Trans on Industrial Electronics 2011;58(10):4583 –92.

[13] Soto WD, Klein S, Beckman W. Improvement and validation of a model for photovoltaic array performance. Solar Energy 2006;80(1):78 – 88.

[14] Wies R, Johnson R, Agrawal A, Chubb T. Simulink model for economic analysis and environmental impacts of a PV with diesel-battery system for remote villages. IEEE Transactions on Power Systems 2005;20(2):692–700.

[15] Esen H, Inalli M, Esen M. A techno-economic comparison of ground-coupled and air-coupled heat pump system for space cooling. Building and Environment 2007;42(5):1955 –65.

[16] Zahedi B, Norum LE. Modeling and simulation of all-electric ships with low-voltage dc hybrid power systems. IEEE Transactions on Power Electronics 2013;28(10):4525–37.

[17] Lan H, Wen S, Hong YY, Yu DC, Zhang L. Optimal sizing of hybrid PV/diesel/battery in ship power system. Applied Energy 2015;158:26 – 34.

[18] Wen S, Lan H, Hong YY, Yu DC, Zhang L, Cheng P. Allocation of ESS by interval optimization method considering impact of

ship swinging on hybrid PV/diesel ship power system. Applied Energy 2016;175:158 –67.

[19] Banaei MR, Alizadeh R. Simulation-based modeling and power management of all-electric ships based on renewable energy generation using model predictive control strategy. IEEE Intelligent Transportation Systems Magazine 2016;8(2):90–103.

[20] Lee KJ, Shin D, Yoo DW, Choi HK, Kim HJ. Hybrid photovoltaic/diesel green ship operating in standalone and grid-connected mode — Experimental investigation. Energy 2013;49:475 –83.

[21] Ovrum E, Bergh T. Modelling lithium-ion battery hybrid ship crane operation. Applied Energy 2015;152:162 –72.

[22] Yao C, Chen M, Hong YY. Novel adaptive multi-clustering algorithm-based optimal ESS sizing in ship power system considering uncertainty. IEEE Transactions on Power Systems 2017;PP(99):1–.

[23] Tsekouras G, Kanellos F. Optimal operation of ship electrical power system with energy storage system and photovoltaics: Analysis and application. WSEAS Transactions on Power Systems 2013;8(4):145–55.

[24] Kanellos FD, Anvari-Moghaddam A, Guerrero JM. A cost-effective and emission-aware power management system for ships with integrated full electric propulsion. Electric Power Systems Research 2017;150:63 – 75.

[25] Ko¨kku¨lu¨nk KYG, Parlak A, Karakas¸ A. Energy cost assessment of shoreside power supply considering the smart grid concept: a case study for a bulk carrier ship. Maritime Policy & Management 2016;43(4):469–82.

[26] Kanellos FD, Tsekouras GJ, Hatziargyriou ND. Optimal demand-side management and power generation scheduling in an all-electric ship. IEEE Transactions on Sustainable Energy 2014;5(4):1166–75.

[27] Aalami H, Moghaddam MP, Yousefi G. Demand response modeling considering interruptible/curtailable loads and capacity market programs. Applied Energy 2010;87(1):243 –50.

[28] Tazvinga H, Zhu B, Xia X. Energy dispatch strategy for a photovoltaic-wind-diesel-battery hybrid power system. Solar Energy 2014;108:412 –20.

[29] Collares-Pereira M, Rabl A. The average distribution of solar radiation correlation between diffuse and hemispherical and between daily and hourly insolation values. Solar Energy 1979;22:155 –64.

[30] Wu Z, Ling R, Tang R. Dynamic battery equalization with energy and time efficiency for electric vehicles. Energy 2017;41:937 –48.

[31] Yang F, Xia X. Techno-economic and environmental optimization of a household photovoltaic-battery hybrid power system within demand side management. Renewable Energy 2017;108:132 –43.

[32] Powell KM, Sriprasad A, Cole WJ, Edgar TF. Heating, cooling, and electrical load forecasting for a large-scale district energy system. Energy 2014;74:877 –85.

[33] Bacher P, Madsen H, Nielsen HA. Online short-term solar power forecasting. Solar Energy 2009;83(10):1772 –83.

[34] Mellit A, Pavan AM. A 24-h forecast of solar irradiance using artificial neural network: Application for performance prediction of a grid-connected PV plant at trieste, italy. Solar Energy 2010;84(5):807 –21.

[35] Suganthi L, Samuel AA. Energy models for demand forecasting–a review. Renewable and Sustainable Energy Reviews 2012;16(2):1223 –40.

[36] Xia X, Zhang J, Elaiw A. An application of model predictive control to the dynamic economic dispatch of power generation. Control Engineering Practice 2011;19(6):638 –48.

[37] Zhang J, Xia X. A model predictive control approach to the

799

13

periodic implementation of the solutions of the optimal dynamic resource allocation problem. Automatica 2011;47(2):358 –62.

[38] Yang H, Wei Z, Lou C. Optimal design and techno-economic analysis of a hybrid solar–wind power generation system. Applied Energy 2009;86(2):163 –9.

[39] Li Q, Wu Z, Xia X. Estimate and characterize pv power at demand-side hybrid system. Applied Energy 2018;218:66 – 77.